

# Evaluation of Fault–Foundation Interaction, Using Numerical Studies



## **Jabbary, M.**

*Msc Student, School of Civil Engineering, Iran University of Science and Technology, Tehran, Iran,*

## **Nabizadeh, A.**

*PhD Candidate, School of Civil Engineering, Iran University of Science and Technology, Tehran, Iran,*

## **Baziar, M. H.**

*Professor, School of Civil Engineering, Iran University of Science and Technology, Tehran, Iran,*

### **SUMMARY:**

Ground movements due to fault rupture are considered as a significant danger affecting manmade structures and facilities. Earthquake fault ruptures may appear at the ground surface causing large differential movements. A few building codes consider fault rupture effects and have rules to protect buildings. This paper applies a finite-element software to simulate dip slip fault (Normal and Reverse) rupture propagation through sandy soil and its interaction effects on foundation systems. The results of numerical studies were verified with centrifuge model experiments, conducted at the University of Dundee (Bransby et al. 2008). Comparison between the numerical and centrifuge model test results shows that there is a fair agreement between numerical and centrifuge data. In contact area between soil and foundation, interface elements with tension cut-off are defined. The results also indicate that the rotation of the foundation is a function of its location relative to the fault rupture and the surcharge load. It is further shown that the presence of a foundation on top of the fault can have a significant influence on the rupture path. Finally, the foundation rotations during fault rupture, the location of the fault outcropping, the vertical displacement of the ground surface and the minimum fault offset at bedrock for the rupture to reach the ground surface were studied.

*Keywords: Finite element software; Fault rupture; Numerical Studies; Verification; Centrifuge Tests*

## **1. INTRODUCTION**

Several engineering structures are destroyed due to foundations displacement during large earthquakes in which fault rupture occurs on surface. Although these structures are designed to resist dynamic loadings, but foundation instability caused by fault rupture leads to structure destruction. Seismic codes such as Eurocode EC8 1994 banned constructing structures adjacent to active faults. However in some situation, construction of structures near faults is inevitable. This situation was seen during the 1999 Taiwan (Chi-Chi) and 1999 Turkey earthquakes.

Field observations (Taylore et al. 1985; Ambraseys and Jackson 1984; Kelson et al. 2001), analytical and experimental research findings (Sanford 1959; Roth et al. 1981; Cole and Lade 1984; Bray et al. 1994a,b; Bray 2001; Johansson and Konagai 2004; Anastasopoulos et al. 2007) have shown that deep and ductile soil deposits may mask a small fault rupture, whereas by contrast with a shallow or “brittle” soil deposit, a large offset in the bedrock will develop a distinct surface fault scarp with almost the same displacement.

Therefore studying effective parameters in damaging foundation by fault rupture is essential to protect structures against fault movement. There are various methods, such as surveying historical events, performing physical tests and numerical modeling to study effective parameters on the direction of fault

rupture. Numerical modeling can be a convenience method of investigating fault direction. However numerical modeling should be validated with some experimental tests. Only when the numerical method is validated, parametric study can be a valuable tool for estimating such phenomena. In this paper, the ABAQUS software which is based on finite element method was implemented for numerical study. Two sets of tests were considered in this paper to verify numerical studies; Normal and Reverse fault-foundation interaction modeled in centrifuge, both conducted by Bransby et al in 2008.

## 2. PROBLEM DEFINITION

Conducted tests geometries are illustrated in figure 1. A strip foundation with assumed load of  $q$  and width of  $B$  is considered on the top of a sand layer with assumed thickness of  $H$  in which a normal fault is located in the right corner of specimen with the distance of  $w$  in foundation interaction tests. Fault displacement (fig.1-a) occurred with the amount of  $h$ , downward, and  $\alpha$  as displacement angle. This set of tests was conducted to study foundation location and load effect on fault rupture direction. As it is illustrated in figure 1b, fault displacement direction is the only difference between normal and reverse fault rupture –foundation interaction tests.

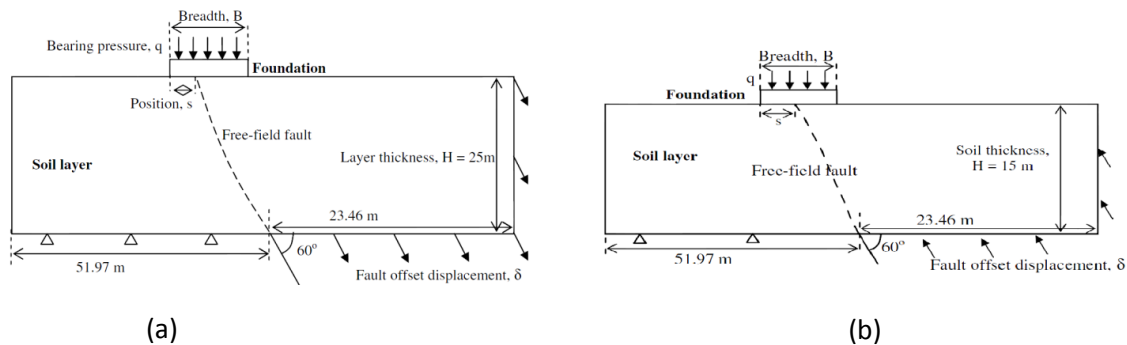


**Figure 1.** Geometry of normal and reverse fault rupture emergence adjacent to a shallow foundation (Bransby et al 2008 a & b)

## 3. EXPERIMENTAL RESULTS

A special apparatus was constructed in the University of Dundee (Bransby et al. 2008) to simulate dip slip faulting and its interaction with strip foundations (Fig.2). The displacing rigid hanging wall base and wall section was supported by a pair of hydraulic jacks which were used for actuation. By pumping oil into the jacks, the block was lifted and a reverse fault was activated; by removing oil from the jacks, the block moved downwards and a normal fault was activated. Three aluminum wedges were installed to impose fault displacement at the desired degree  $60^\circ$ . Images of the deformed soil specimen at different bedrock displacements were captured using a digital camera. Vertical and horizontal displacements at different positions within the specimen were computed through image processing and measured directly at several points on the surface using linearly variable differential transformers. Displacement profiles and shear strain contours were also computed through additional post processing.

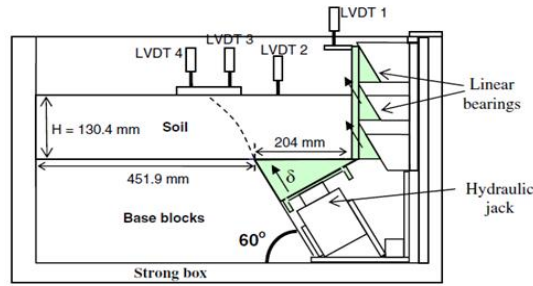


**Figure 2.** General test template in centrifuge condition (Bransby et al 2008 a & b)

It should be noted that experimental modeling performed using centrifuge instrument with 115-g and mentioned dimensions were calculated after dimensional analysis in 1-g condition. Test specifications with presence of foundation are listed in Table (3.1):

**Table 3.1** Basic parameters and prototype dimension of centrifuge tests with presence of foundation (Bransby et al 2008)

Normal Fault rupture				Reverse Fault rupture			
Test Number (Numbered by Bransby)	s (m)	q (kPa)	B (m)	Test Number (Numbered by Bransby)	s (m)	q (kPa)	B (m)
14	2.9	91	10	29	5.9	90	10
15	3.0	37	10	30	5.9	37	10
18	8.1	91	10	19	0.8	90	10
20	10.5	91	25	21	8.28	90	15

Free field tests were conducted with Fontainebleau sand in 60% relative density with 25m height in normal fault and 15m height in reverse fault which was illustrated in figure 1 in prototype scale.

A rigid foundation with 10m width was located on soil surface. Foundation position and surcharge load effect on fault rupture path were surveyed. 10m width foundations were substituted with 25m width foundations for normal fault and 15m for reverse fault to investigate foundation width effect on faulting direction.

Free field tests (Tests 12 and 28) were performed with presence of foundation to determine fault rupture location in order to calculate S parameter for following tests.

In tests 14 & 29, the width of foundation, B=10m and bearing pressure q=91kPa, (equal to a 9 story building) were located on sand with S=2.9m for normal faulting and S=5.9m for reverse faulting. Fault displacement was applied to investigate the effect of horizontal displacement of fault on foundation rotation in test number 29 and also in test number 14 the effect of vertical displacement of fault on horizontal displacement of foundation was investigated.

Tests 15 & 30 were performed to determine effect of bearing pressure on fault rupture direction. So the only difference between these tests and two previous tests was bearing pressure which was changed to 37 kPa.

In Tests 18 & 19, effect of foundation position on fault rupture path was studied. So foundation location was changed from S=3m in previous test to 8.1m and from S=5.9m in previous test to S=0.8m for normal and reverse tests respectively, while foundation pressure remained at 91kPa.

Tests number 20 and 21 were performed to study foundation width effect on normal and reverse fault rupture direction. Foundation location in these tests were changed beside foundation width as S=10.5m in test number 20 and S=8.28m in test number 21.

#### 4. NUMERICAL MODELING METHOD:

In this study, the Finite Element software was implemented for numerical studies. Mohr-Coloumb constitutive model has been used to simulate the softening behavior of soil and next the equation presented by Anastopoulos (2007) has been applied. In this equation, demonstrated in Equation (4.1), soil friction and dilation angles, which are as a function of plastic shear strain, are reduced

$$\varphi_{mob} = \begin{cases} \varphi_p - \frac{\varphi_p - \varphi_{res}}{\gamma_f^p} \gamma_{oct}^p & \text{for } 0 \leq \gamma_{oct}^p < \gamma_f^p \\ \varphi_{res} & \text{for } \gamma_{oct}^p \geq \gamma_f^p \end{cases} \quad (1)$$

$$\psi_{mob} = \begin{cases} \psi_p \left(1 - \frac{\gamma_{oct}^p}{\gamma_f^p}\right) & \text{for } 0 \leq \gamma_{oct}^p < \gamma_f^p \\ \psi_{res} & \text{for } \gamma_{oct}^p \geq \gamma_f^p \end{cases} \quad (2)$$

As seen in equation (1)  $\varphi_p$  and  $\varphi_{res}$  are ultimate friction and residual friction angles. Moreover, in equation (2),  $\psi_p$  is equal to the ultimate dilation angle and  $\psi_{res}$  is equal to the plastic octahedral shear strain ( $\gamma_{oct}^p$ ) at which softening has been completed. The thickness of the shear zone was found to be depended on mesh size [Anastasopoulos et al 2009].

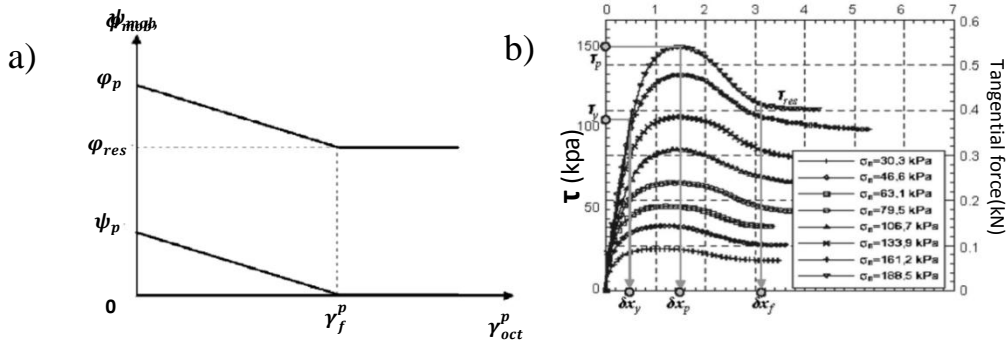


**Figure 3.** a) Demonstration of changes of friction and soil dilation due to shear plastic strain b) Behavior of Fontainebleau sand in direct shear tests under different stresses

In the numerical model, foundation has been modeled as a linear elastic element with high rigidity and thickness of 1 meter. It should be noted that boundary condition has been chosen such that there is no need to model bedrock (foam block test machine), after applying the gravitational acceleration and loading the foundation on soil, fault displacement is moving the right boundary of soil.

In the contact surface between soil and foundation, the normal contact and frictional contact with the friction coefficient of  $0.7tg(\varphi)$  has been used. The gap element specification has been applied to model the lost contact between the soil and foundation.

#### 4.1. Faulting Modeling in Free Field Condition

To simulate faulting in the FE software, strain softening behavior which can have clear impact on mesh relocation changes should be applied. Regarding to this cause, Anastopoulos 2007 equation was applied to correct calculation of soil resistance in the rupture propagation zone.

Although, modeling the crack in FE code is left as a function of mesh size, but created model in numerical study was able to successfully estimate the position of surface displacement in two modes of normal faulting and reverse faulting.

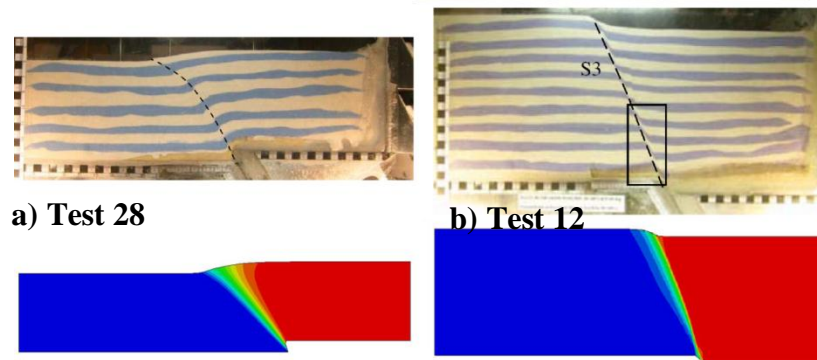


**Figure 4.** Comparison between experimental and numerical modeling in test number 12 (Figure 4b) and test number 28 (Figure 4a)

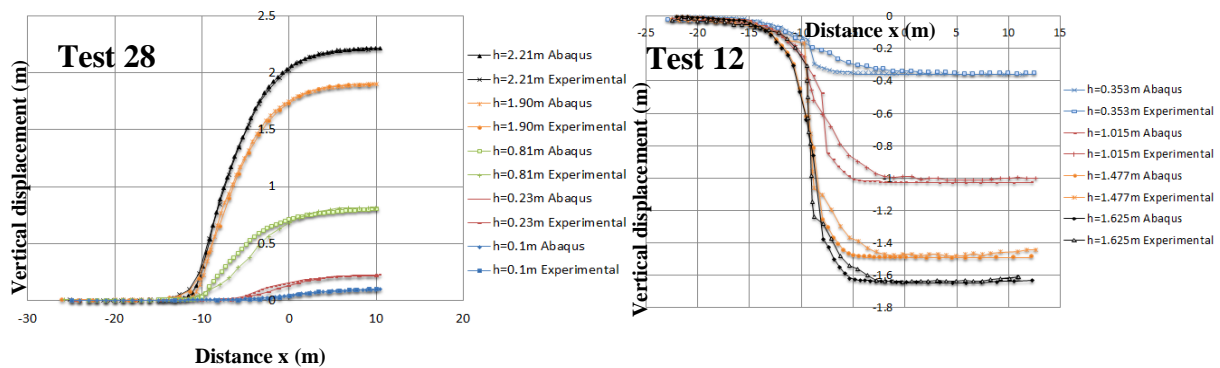


**Figure 5.** Surface displacement comparison in numerical modeling and experimental test (test number 12 and 28) Critical parameters in modeling these tests could be  $\varphi_p=35$  and  $\varphi_{res}=30.2$  and  $\psi_p=6$  and  $\gamma_f^p = 0.244$  which were predicted in Anastapolous equation (2007) for Fontainebleau sand. The prediction of numerical analysis for vertical displacement at the soil surface in both normal faulting and reverse faulting were demonstrated in figure 4 and in figure 5 along with displacement observed from experimental tests for several different fault displacements.

#### 4.2. Numerical Modeling of Fault Rupture with the Presence of Foundation

As it could be seen in figure 6b, presence of foundation in normal faulting led to rupture propagation diversion toward footing-wall and foundation along with bottom soil were collapsed toward hanging-wall. Regarding to the experiment 29 as shown in figure 6a, presence of foundation caused that part of the soil in free field and located within hanging-wall, stayed with no motion in footing-wall.

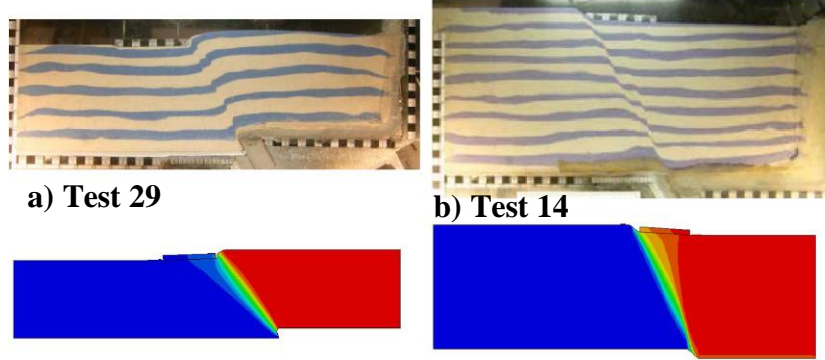


**Figure 6.** Comparison between experimental and numerical modeling in test number 14 (Figure 6b) and test number 29 (Figure 6a)

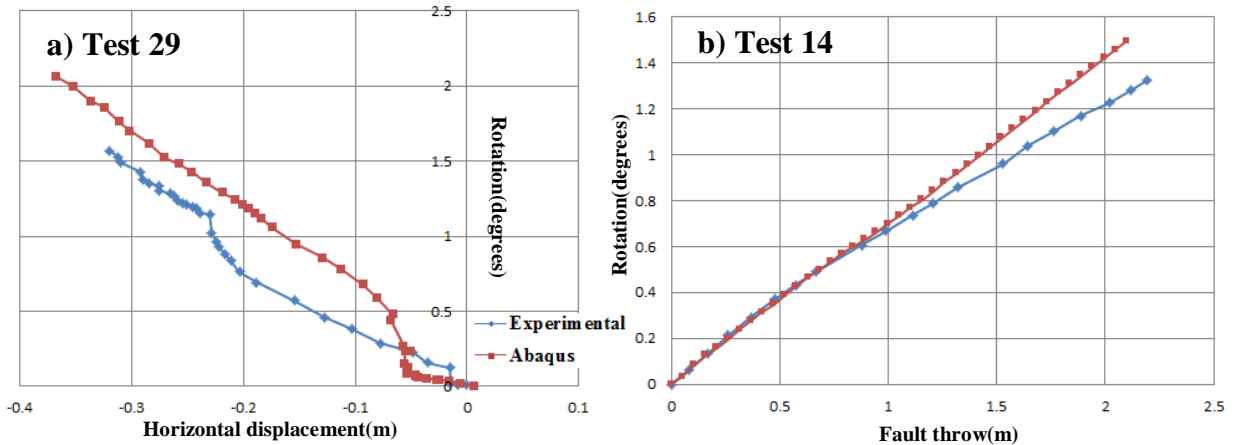


**Figure 7.** The effect of vertical displacement of fault on horizontal displacement of foundation in test number 14 and the effect of horizontal displacement of fault on foundation rotation in test number 29

The impact of horizontal displacement of foundation on the rotation of foundation in test 14 and also the impact of vertical displacement of fault on the rotation of foundation in test 29 were shown in figure 7.

#### 4.3. Interaction with Shallow Foundation (Test Number: 15 and 30)

Regarding to the reduction of applied load from 91kPa to 37kPa, as seen from Figs 8b and 6b, downward displacement of the left side of foundation, caused by normal faulting, reduced and the foundation rotation increased. Also, regarding to the reverse faulting, it is evident from figure 8a and figure 6a, reduction of applied load from 91kPa to 37kPa caused the displacement of right corner of the foundation to move upward and existence of plastic zone under the foundation. The results of these two tests with vertical displacement of the fault on the rotation of foundation were shown in Figure 9.

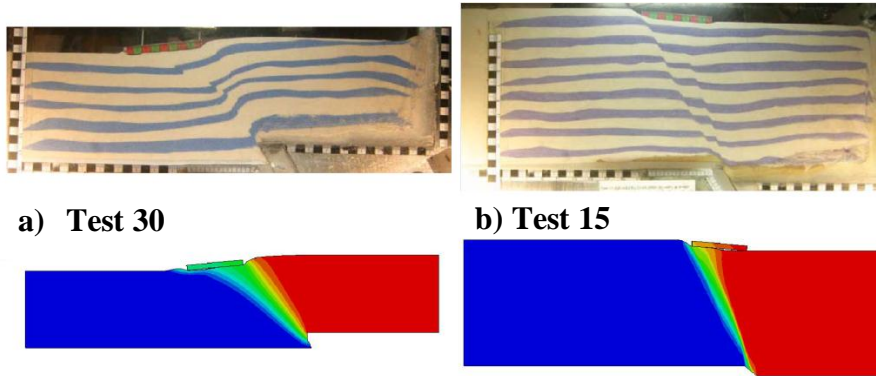


**Figure 8.** Comparison between experimental and numerical modeling in test number 15 (Figure 8b) and test number 30 (Figure 8a)

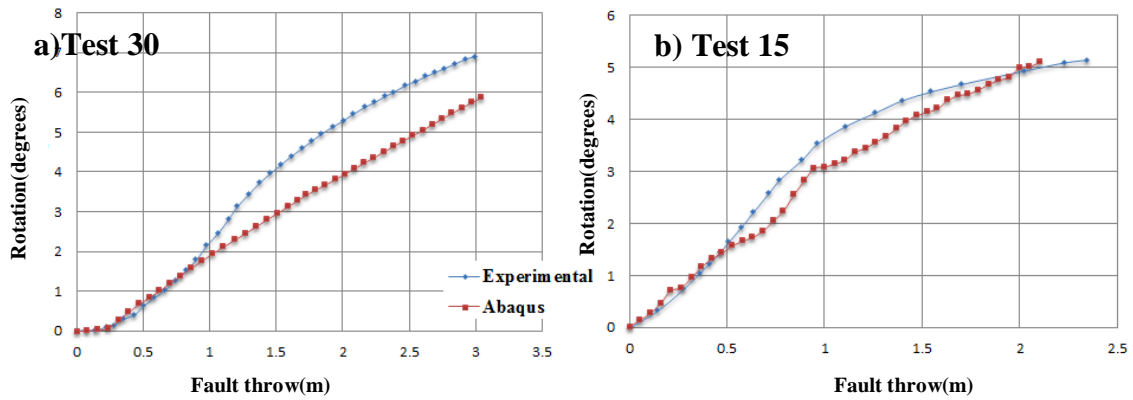


**Figure 9.** Foundation rotation variation due to vertical displacement of foundation in test number 15 (Figure 9a) and test number 30 (Figure 9b)

#### 4.4. Interaction with Shallow Foundation (Test Number: 18 and 19):

In test 18, changing the position of the foundation toward the footing-wall led to the higher resistance of foundation in front of downward slide. For this reason, rotation of foundation was greater than rotation seen in test 14.

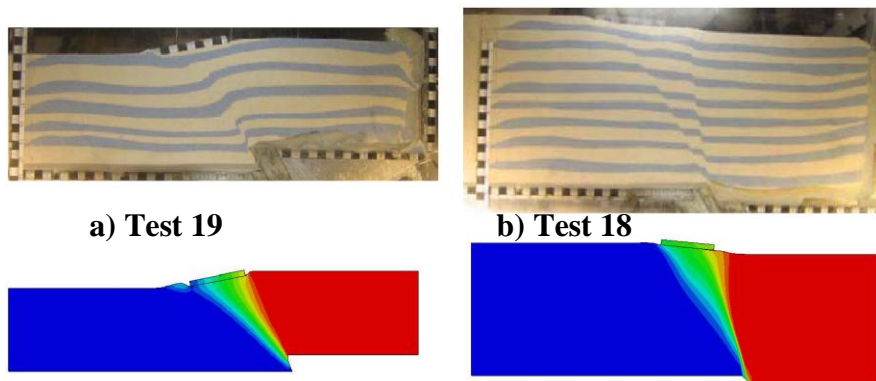


**Figure 10:** Comparison between experimental and numerical modeling in test number 18 (Figure 10b) and test number 19 (Figure 10a)

Changing the position of foundation toward hanging-wall led to upward displacement of the right corner of the foundation while the left side of the foundation stayed at footing-wall. It should be noted that this difference of displacement under the foundation led to increase the rotation of foundation more than test 29 (figure 10). The graph of rotation changes of foundation due to vertical fault displacement is presented in figure 11.

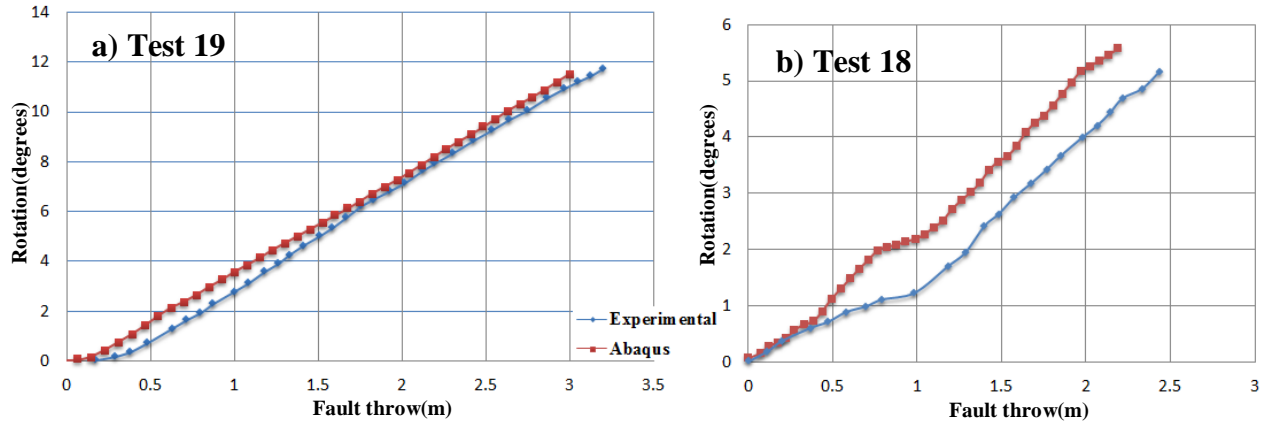


**Figure 11.** Foundation rotation variation due to vertical displacement of foundation in test number 18 (Figure 11b) and test number 19 (Figure 11a)

#### 4.5. Fault rupture modeling with presence of foundation (Test number: 20 and 21)

The rotation of foundation in front of vertical fault displacement for both numerical and experimental studies was shown in figure 13.

These two tests had different impacts on determining the fault direction. In test 20, direction of fault rupture was completely distributed under the foundation while in test 21 faulting were visible in the right side area of the foundation. The differences between these two tests were shown in Figure 12.

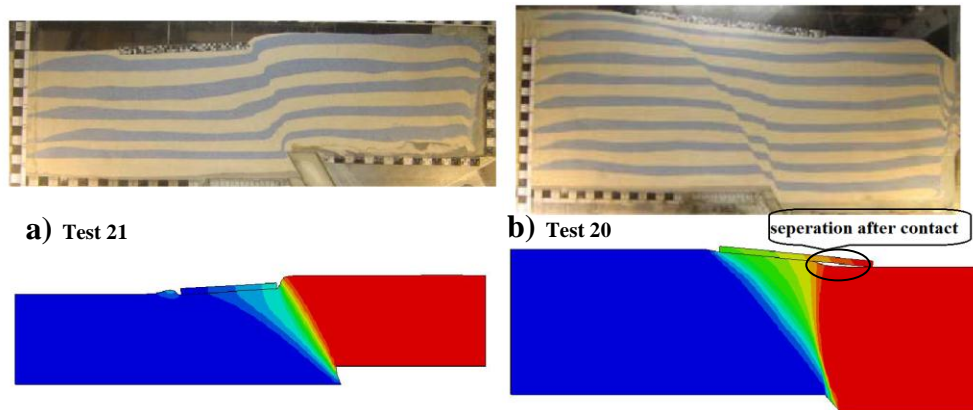


**Figure 12.** Comparison between experimental and numerical modeling in test number 21 (Figure 12a) and test number 20 (Figure 12b)

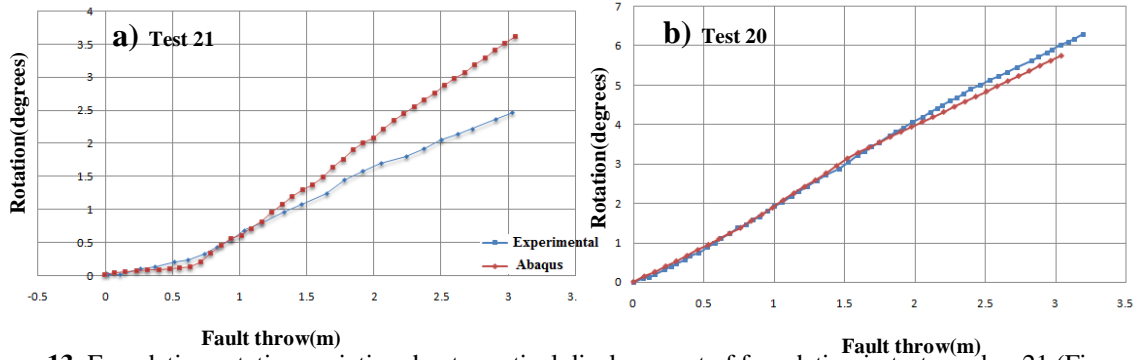


**Figure 13.** Foundation rotation variation due to vertical displacement of foundation in test number 21 (Figure 13a) and test number 20 (Figure 13b)

## 5. CONCLUSION

Results of this study draw the following points:

- 1- Numerical studies could correctly predict the direction of the fault rupture pattern, the amount of differential displacement of surface and also rotation of foundation.
- 2- Increasing the surcharge load ( $q$ ) on normal and reverse faulting will lead the direction of fault to move away from the foundation, and will result in decreasing the rotation of the foundation.
- 3- In the numerical modeling, performed in this paper, ABAQUS Explicit analysis has been used which was compared to ABAQUS standard analysis, allows to have more movement of meshes without need for re-meshing requirement. It should be noted that re-meshing method will reduce the accuracy of the FEM software. However, in some models built in ABAQUS software (test 14 and 15 and 21) which changes of displacement is focused in a limited area like a crack, fault displacement of the numerical studies is different with the results of experimental tests.
- 4- As it had been already mentioned, in the software base on FEM and continuum mechanics, crack modeling depends on mesh size (Walters and Thomas, 1982) and this differences increase with fault displacement. The difference between experimental and numerical results reduces with increasing displacement.
- 5- As seen in figure 12b, fault displacement would cause to create an uncontact zone between soil and foundation. As it is clear from the comparison of experimental and numerical diagrams (figure 13b), ABAQUS software would present results very similar to experimental model despite modeling this detachment
- 6- Finally, position of foundation regarding to the fault should be considered as an important parameter in foundation design. In normal faulting, the changing location of foundation toward footing-wall would cause the downfall of soil towards hanging-wall, and as a result it will increase the foundation rotation. Regarding to reverse faulting, changing the location of foundation toward hanging wall would lead downfall of soil towards footing-wall and will cause increase of foundation rotation.

## REFERENCES

- ABAQUS. \_2010\_. ABAQUS V.6.10 user's manual, Providence, R.I.
- Ambraseys, N., and Jackson, J. \_1984\_. "Seismic movements." Ground movements and their effects on structures, P. B. Attewell and R. K. Taylor, eds., Surrey Univ. Press, Surrey, U.K., 353–380.
- Anastasopoulos, I., Gazetas, G. (2007a). foundation-structure systems over a rupturing normal fault: Part I. Observations after the Kocaeli 1999 earthquake." Bulletin of Earthquake Engineering, 5 (3), pp. 253-275.
- Anastasopoulos, I., Gazetas, G, M. ASCE; Bransby, F., Davies, M.C.R; and El Nahas, A. (2009). "Normal Fault Rupture Interaction with Strip Foundations." Journal Of Geotechnical And Geoenvironmental Engineering.
- Bransby, F., Davies, M.C.R., El Nahas, A., Nagaoka S., (2008). "Centrifuge modeling of normal fault-foundation interaction." Bulletin of Earthquake Engineering, Special Issue: Integrated approach to fault rupture- and soil-foundation interaction, Vol.6, No.4, pp.607-628.
- Bransby, F., Davies, M.C.R., El Nahas, A., Nagaoka S., (2008). "Centrifuge modeling of reverse fault-foundation interaction." Bulletin of Earthquake Engineering, Special Issue: Integrated approach to fault rupture- and soil-foundation interaction, Vol.6, No.4, pp.585-605.
- Bray, J. D. \_1990\_. "The effects of tectonic movements on stresses and deformations in earth embankments." Ph.D. thesis, Univ. of California, Berkeley.
- Bray, J. D. \_2001\_. "Developing mitigation measures for the hazards associated with earthquake surface fault rupture." Proc., Workshop on Seismic Fault-Induced Failures—Possible Remedies for Damage to Urban Facilities, 55–79.
- Bray, J. D., Seed, R. B., Cluff, L. S., and Seed, H. B. \_1994a\_. "Earthquake fault rupture propagation through soil." J. Geotech. Engrg., 120\_3\_, 543–561.